Pergamon

Tetrahedron 56 (2000) 8419–8427

TETRAHEDRON

Hydrogen Bonding Control of Molecular Self-Assembly: Aggregation Behavior of Acylaminopyridine–Carboxylic Acid Derivatives in Solution and the Solid State

Abdullah Zafar,[a] Steven J. Geib,[a] Yoshitomo Hamuro,[a] Andrew J. Carr[b] and Andrew D. Hamilton[b,*]

[a]*Department of Chemistry, University of Pittsburgh, Pittsburgh, PA 15260, USA*
[b]*Department of Chemistry, Yale University, New Haven, 225 Prospect Street, Connecticut, CT 06520, USA*

Received 6 July 2000; accepted 22 August 2000

Abstract—In this paper we report the design, synthesis and investigation of a family of acylaminopyridine–carboxylic acid monomers that can aggregate through bidentate hydrogen bonding interactions between the carboxylic acid and the aminopyridine sites. We show that in solution the nature of the aggregate depends on the substitution pattern of the monomer and present evidence from NMR and mass spectrometry that in some cases cyclic association occurs.

Introduction

The development of small organic components that can form large molecular aggregates through non covalent interactions has been an active area of research over the past decade.[1] Potential applications for these types of controlled assemblies lie in such areas as non-linear optical materials, liquid crystals and catalysis.[2] A key to the development of such systems is to control the structure of the final supramolecular assembly. Another important requirement is the possibility of functionalization on the self-assembling template without disturbing the supramolecular structure.[3]

We have shown that bis-aminopyridines can bind to bis-carboxylic acids through a double bidentate hydrogen bonding interaction to form 1:1 complexes (as in Fig. 1a).[4] The length of the spacer determines the nature of the complex and in certain cases 2:2 aggregates can be formed.[5] As part of a program aimed at using hydrogen bonding to control self-assembly, we were interested in probing the design of components containing both carboxylic acid and aminopyridine groups within the same framework. Our hope was that such molecules would self-assemble in non-polar solvents (as in Fig. 1b) with the shape and size of the aggregate controlled by the relative positioning of the two hydrogen bonding groups. The simplest derivative in this class would involve substituting a carboxylic acid group on 2-acylaminopyridine at different positions, as in **1** and **2**. The advantage in this design is the simplicity of the monomer subunit and the relatively easy functionalization of the amine nitrogen. The resulting self-complementary derivatives can self-associate through bidentate hydrogen bonding interactions to form dimers (**3** and **4**) with very different dispositions of the carboxylic acid and acylaminopyridine

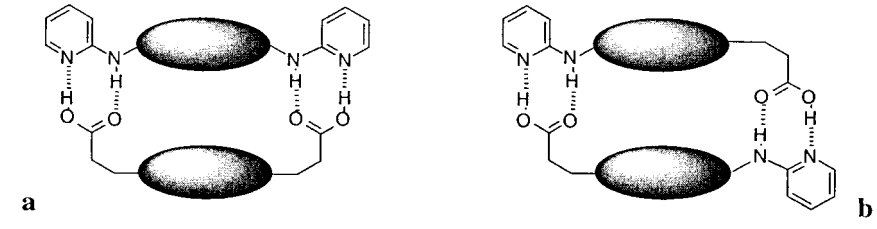

Figure 1. (a) Host–guest interaction between bis-carboxylic acid and bis-acylaminopyridine. (b) Potential aggregation of acylaminopyridine–carboxylic acid derivatives.

Keywords: self-assembly; hydrogen bonding; acylaminopyridine–carboxylic acid.
* Corresponding author. Tel.: +1-203-432-5570; fax: +1-203-432-3221; e-mail: andrew.hamilton@yale.edu

0040–4020/00/$ - see front matter
PII: S0040-4020(00)00733-X

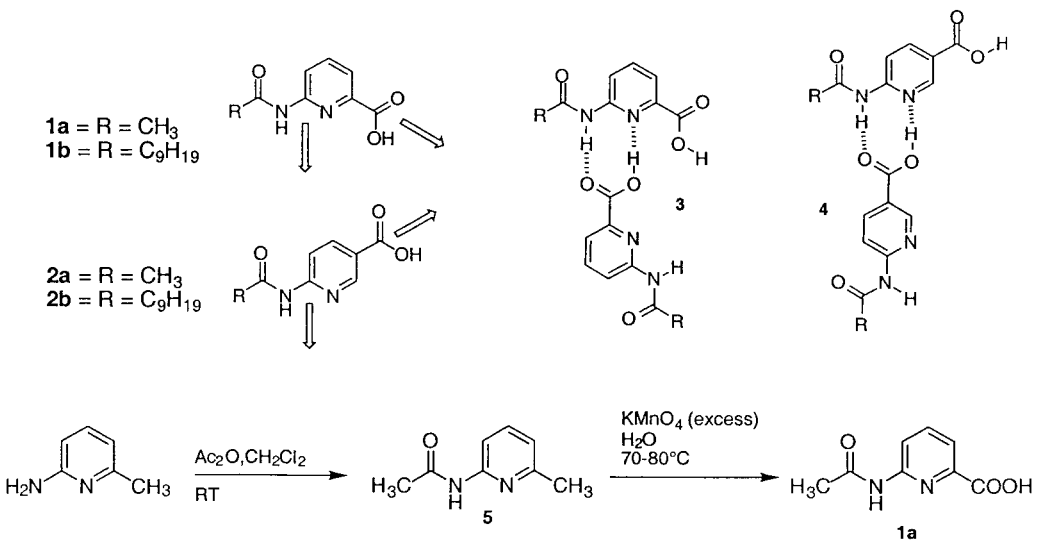

Scheme 1.

functionalities. These in turn can potentially form a range of linear or cyclic molecular aggregates. In this paper we report the synthesis, X-ray crystal structures and aggregation properties of a family of acylaminopyridine–carboxylic acids and show that the nature of the aggregate is determined by the relative orientation of the two interacting groups.

Results and Discussion

Synthesis

The acylaminopyridine–carboxylic acid derivatives could be prepared by two primary routes. The first involved acylation of the aminopicoline followed by oxidation of the

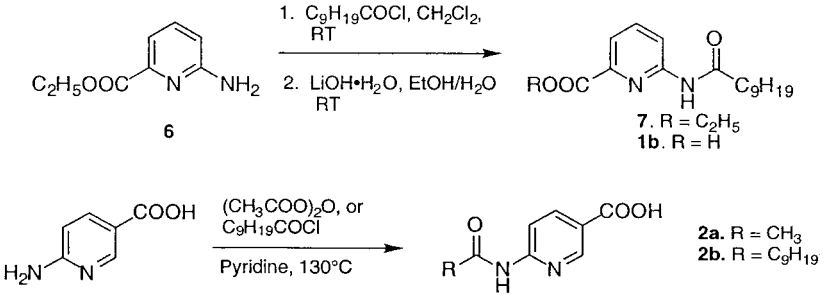

Scheme 2.

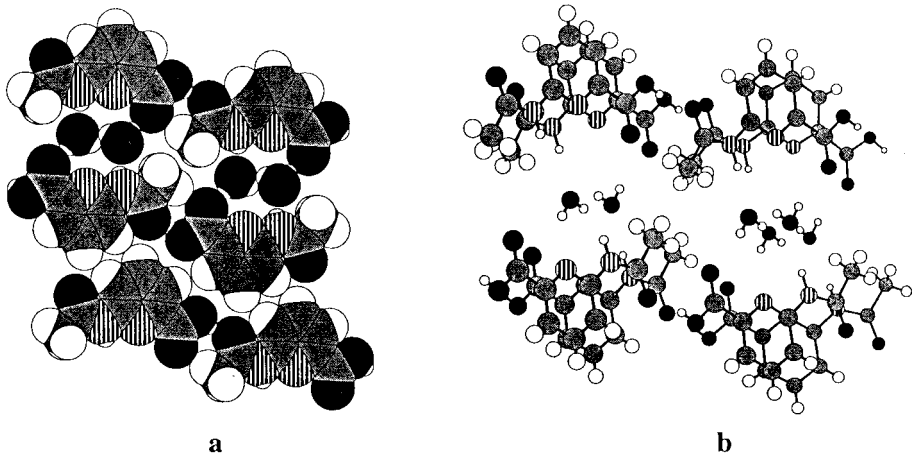

Figure 2. (a) Space filling representation of the X-ray crystal structure of **1a** showing the hydrogen bonding pattern within a layer. (b) Three dimensional packing in **1a**.

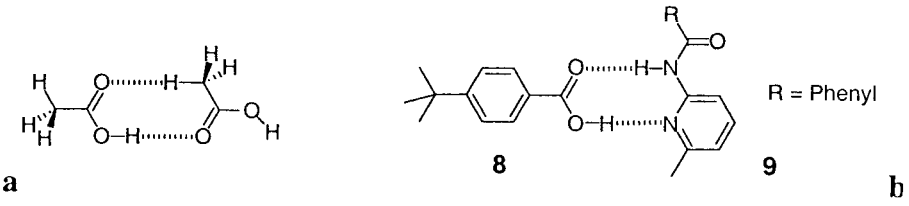

Figure 3. (a) Acetic acid dimer, (b) Intermolecular complex between **8** and **9**.

methyl group to the corresponding carboxylic acid. For example, acylaminopyridine **1a** was synthesized by acylating 2-amino-6-picoline with acetic anhydride followed by oxidation with potassium permanganante (Scheme 1). Alternatively, direct acylation of the aminopicolinic acid or ester could be used in certain cases. Acylaminopyridine **1b** was synthesized in three steps via esterification of 6-aminopicolinic acid followed by acylation with decanoyl chloride and basic hydrolysis (Scheme 1). Aminopyridines **2a** and **2b** were synthesized in a single step by acylating 6-aminonicotinic acid with acetic anhydride and decanoyl chloride respectively (Scheme 2).

Solid state structures

Acid **1a** was not soluble in chloroform. However, we were able to grow X-ray quality crystals from a mixture of methanol and water. The most striking feature of the crystal structure is the absence of the expected bidentate hydrogen bonding pattern between the aminopyridine and the carboxylic acid groups. The aminopyridines pack in a linear fashion by forming hydrogen bonds between the amide carbonyl and the carboxylic acid OH (C=O···H–O, dist. 1.82 Å) as shown in Fig. 2a. The linear ribbons face each other in an antiparallel arrangement and the individual units are connected together by two water molecules. The water dimer forms four hydrogen bonds to the two aminopyridine units (NH···OH_2, 2.06 Å; C=O···HOH, 2.03 Å). Another interesting feature is the CH···O interaction (CH···O, 2.33 Å) between the acetyl CH_3 and the acid carbonyl groups. This type of bidentate hydrogen bonding interaction between acetyl and carboxylic acid groups has also been found in the crystal structure of acetic acid (OH···OC, 1.64 Å, CH···OC, 2.4 Å), as shown schematically in Fig. 3a.[6] Fig. 2b shows the stacking of layers to form the lattice in **1a**. The distance between the layers is 4.9–5.1 Å.

Acid **2a** was found to be sparingly soluble in most organic solvents. However, we were able to grow X-ray quality crystals from a solution of **2a** in water at 38°C. The X-ray crystal structure shows a bidentate hydrogen bonding pattern between the aminopyridine and the carboxylic acid groups that form linear tapes (NH···O=2.03 Å, OH···N=1.75 Å) (Fig. 4a). The structure is nearly planar and the out of plane bending of both the amide and the carboxylic acid group is within 5°. There is close packing between the two adjacent antiparallel linear tapes with close positioning of the amide carbonyl and the hydrogen at C-4 of the pyridine ring (CO···HC-4=2.38–2.47 Å). Fig. 4b shows the three dimensional packing in which the linear tapes stack over each other. The interlayer distance ranges from 4.9–5.1 Å.

Solution studies

Acid 1b. It is known that amides are self-complementary through NH···OC interactions and this feature has been used to form hydrogen-bonding aggregates.[7] The absence of any bidentate hydrogen bonding in the crystal structure of **1a** raised the need to establish the nature of self-association in solution. NMR dilution experiments on **1b** were performed in $CDCl_3$ over a concentration range of 0.1 mM to 100 mM. The amide N–H shifted downfield from 7.8 ppm at 0.16 mM to 10.36 ppm at 95.9 mM (Fig. 5). A corresponding dilution experiment with ester **7**, which is incapable of bidentate hydrogen bonding, showed a small downfield shift of the amide N–H resonance indicating little self-association in solution.

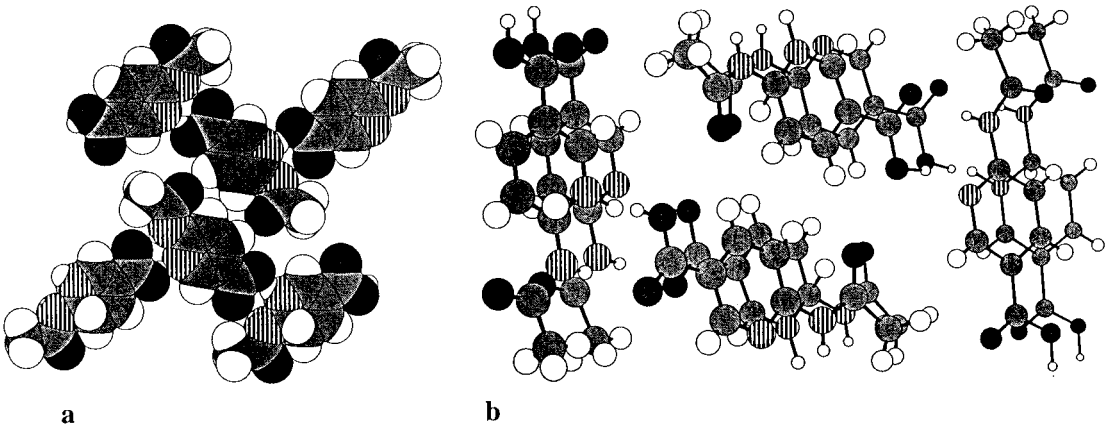

Figure 4. X-ray crystal structure of **2a**. (a) Hydrogen bonding layer arrangement. (b) The three dimensional packing in **2a**.

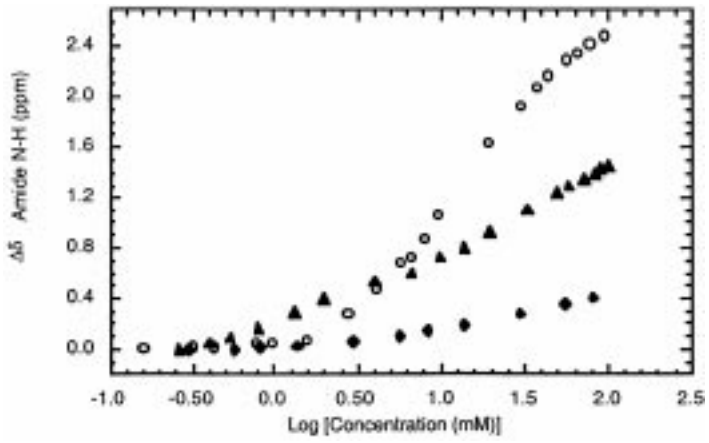

Figure 5. The amide N–H NMR shift in $CDCl_3$ against Log[Conc. mM] for **1b** (○), **7** (◆) and **8** and **9** (1:1, ▲).

The difference of more than 2 ppm in the downfield shift of the amide N–H groups of **1b** and **7** at 100 mM clearly indicates that the presence of carboxylic acid is essential for the aggregation of **1b**. The size of the downfield shift (>2.5 ppm) and the sigmoidal shape of the curve for **1b** suggest the formation of a hydrogen-bonded complex at high concentration with dissociation occurring at or below 1 mM. The nature of the self-associated species can be investigated by using the Saunders and Hyne analysis of molecular aggregation.[13] This model assumes that at equilibrium only two dominant species, the monomer (M) and the most stable oligomeric species (N) are present in solution:

$$nM \overset{K}{\rightleftharpoons} N \qquad K = \frac{N}{M^n}$$

The molar ratio of the monomer, $X=M/M_0$, is obtained using the equation: $M_0=XM_0+nKX^nM_0^n$, where M_0 is the original concentration of the monomer. The chemical shift is then calculated by using: $\delta_{calcd}=\delta_M X+\delta_N(1-X)$, where δ_M is the chemical shift of the monomer and the δ_N is the chemical shift of the oligomer. Non-linear curve fitting can then be carried out for different values of n, which represents the number of monomers involved in the most stable oligomeric complex. Finally, for each curve fit the chi square value is calculated by using the expression: $\chi^2 = \sum(\delta_{calcd} - \delta_{obs})^2$.

Saunders and Hyne analysis of the dilution curve for **1b** provides the best fit at aggregation number 'n'=3. The curve fit for the monomer–trimer model is shown in Fig. 6. Detailed results of the curve fitting analysis for different aggregation numbers are listed in Table 1.

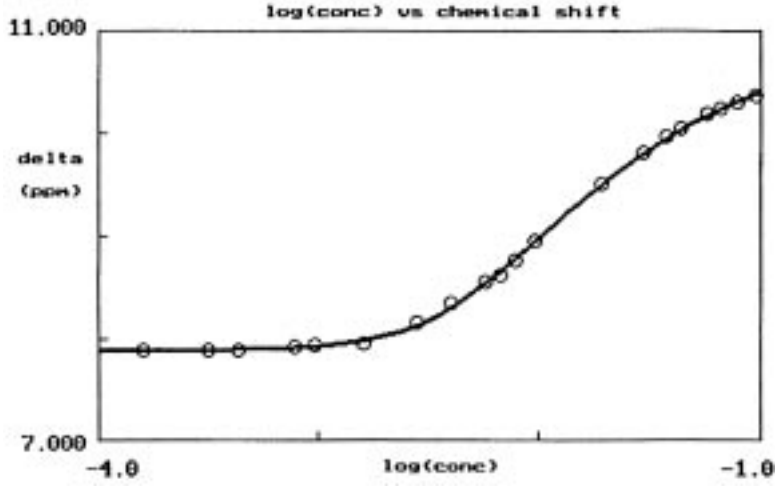

Figure 6. ^{1}H NMR dilution curve obtained for **1b** in $CDCl_3$, (○) experimental; (—) curve fitting for n=3.

Table 1. Results of non-linear curve fitting

Aggregation number 'n'	Aggregation constant (K_n)	Monomer shift δ_m (ppm)	Oligomer shift δ_n (ppm)	$\chi^2\times10^{-3}$
2	27 M^{-1}	7.75	11.95	101.9
3	4474 M^{-2}	7.88	10.95	7.46
4	7.28×10^5 M^{-3}	7.92	10.70	37.3
5	1.2×10^8 M^{-4}	7.94	10.59	82.6

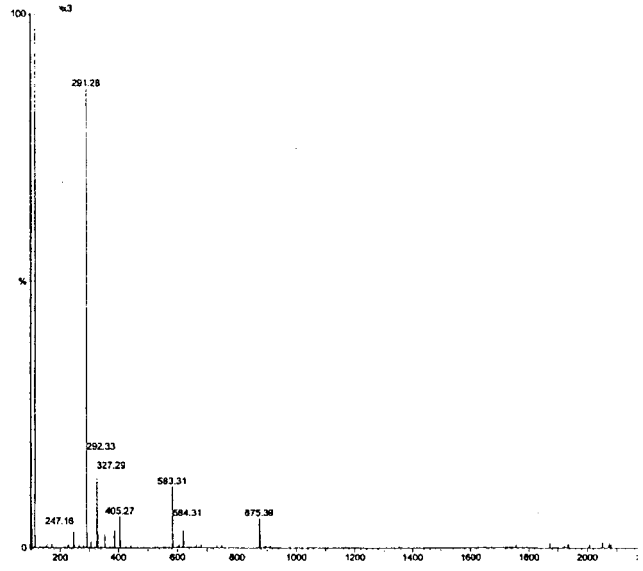

Figure 7. ESMS of **1b** in methanol.

Electrospray mass spectrometry in positive ion mode was performed using methanol as a solvent but gave no $[M+1]^+$ peaks. However, in the negative ion mode there were three distinct peaks corresponding to M−1 (*m/e* 291.28), 2M−1 (*m/e* 583.31) and 3M−1 (*m/e* 875.39) (Fig. 7). The absence of any higher oligomers in the ESMS spectrum strongly suggests that the trimeric and dimeric aggregates are formed preferentially in the gas phase.

Nature of the trimeric aggregate

The NMR experiments described above point to a bidentate hydrogen bonding interaction for the association of **1b**, as in **3**. However, further oligomerization to the trimeric species indicated by the curve fitting and ESMS experiments can occur to give either a cyclic or linear aggregate. Energy minimized structures for cyclic and linear forms of the trimer are shown in Fig. 8. In both cases undistorted bidentate hydrogen bonds are observed between the aminopyridine and the carboxylic acid groups (N–H···O, 1.7 Å; OH···N, 1.9–2.0 Å). Cyclic aggregates should be favored over the corresponding linear form,[8] since $2n-2$ hydrogen bonds are formed in the latter but $2n$ in the former. Also, in the cyclic aggregate a planar arrangement of the components is possible whereas in the linear form steric interaction of the alkyl substituents forces non-planarity.

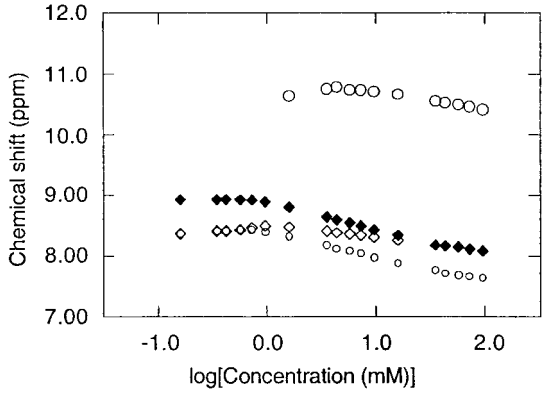

Figure 9. The ^{1}H chemical shifts vs. log[**2b**] for H2 (◆); H4 (◇), H5 (○) and the amide-N–H (o) in $CDCl_3$.

Further support for the cyclic complex comes from a comparison (Fig. 5) of the chemical shift dependence on concentration between **1b** (containing both hydrogen bonding groups within the same molecule) and a 1:1 mixture of benzoic acid **8** and acyl aminopyridine **9** (in which the interacting groups are in separate molecules; Fig. 3b). In the latter situation no cyclization is possible and the chemical shift changes would be expected to mirror those of the linear aggregate rather than the cyclic form. Fig. 5 shows differences in both the shape of the dilution curve and the size of the chemical shift changes for **1b** compared to **8**+**9**. At 100 mM concentrations the $\Delta\delta$ for the amide-NH of **1b** is twice that of **8**+**9**, suggesting the formation of a more stable entity in the case of **1b**. This increased stability is also reflected in the sigmoidal shape of the dilution curve for **1b** which contrasts with the steady change for **8**+**9**. While not conclusive, the different behavior of **1b** compared to **8**+**9** indicates the formation of a cyclic aggregate in solution.

Acid 2b. A dilution experiment for **2b** in $CDCl_3$ over a concentration range of 0.16 mM to 96 mM is shown in Fig. 9. The amide N–H showed a small upfield shift (Fig.

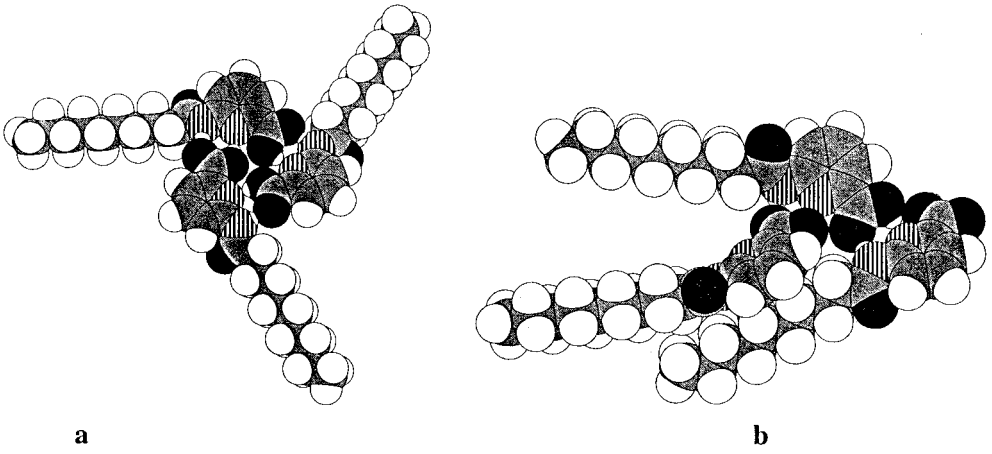

Figure 8. Energy minimized structures of two possible trimers of **1b**.[9] (a) Cyclic trimer. (b) Linear tape.

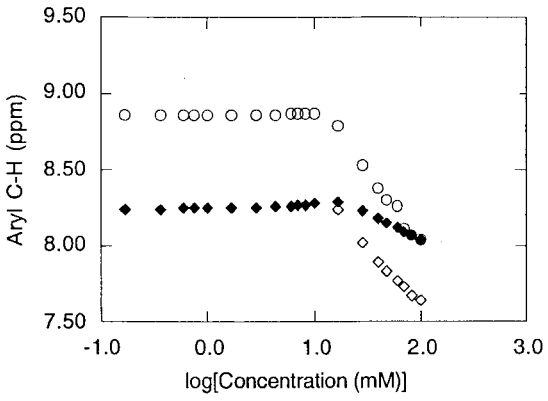

Figure 10. The ^{1}H chemical shifts vs log[**2b**] for H2 (○); H4 (◆), and H5 (◇) in 2% DMSO-d_6/98% $CDCl_3$ (V/V).

9) with increasing concentration in sharp contrast to the large changes that occurred with the isomeric 2,6-disubstituted derivative **1b**.[10]

At 96 mM the chemical shift of the amide-N–H in **2b** matches exactly that of **1b**. Therefore, it appears that the amide N–H in **2b** is strongly hydrogen bonded over the entire concentration range and that the hydrogen bonded aggregate is very stable in chloroform. There is also an upfield shift of the protons on the pyridine ring with increasing concentration above 10 mM (Fig. 9). These aromatic proton shifts in the absence of amide N–H shifts indicate higher order association of the stable hydrogen bonded aggregate presumably through π-stacking interactions (no pyridine-H shifts are seen with **7** or **8**+**9**). Saunders and Hyne analysis of the pyridine-2H shift (as described above) gave a best fit for the monomer–trimer model and an association constant of $22.49\times10^3\ M^{-2}$ (Fig. 11). This type of π-stacking aggregation has previously been observed by Moore and Zhang in the dimerization of hexa-(phenylacetylene) macrocycles in chloroform[11] and also by us, in both the solid state and solution, with 5-alkoxyisophthalic acid derivatives.[12]

In order to reduce the stability of the hydrogen bonded aggregate of **2b**, we performed another dilution experiment in the more polar conditions of 2% DMSO-d_6/98% $CDCl_3$ (V/V). In this case the amide-N–H resonance shifted from 8.6 ppm at 0.17 mM to 10.16 ppm at 100.9 mM (Fig. 12). The shift of more than 1.5 ppm as well as the sigmoidal shape of the curve indicated the formation of a well defined hydrogen bonded aggregate at high concentration. Again, upfield shifts were seen for the pyridine-H resonances above 10 mM (Fig. 10). However, unlike the N–H shifts, the aromatic-H shifts did not show saturation at high concentration, indicating that they are due to a higher order π-stacking aggregation and not as a result of the bidentate hydrogen bonding.

The presence of both hydrogen bonding and π-stacking aggregation with **2b** renders Saunders–Hyne analysis of the amide N–H dilution curve imprecise, as the single equilibrium model no longer applies. The results of curve fitting to different aggregation numbers are summarized in Table 2. The best fit (Fig. 12) was obtained for the monomer–pentamer model. Although, the quality of the fit is poor due to the multiple aggregation phenomena the results point to aggregation properties of **2b** that are very different from those of **1b**. In particular, a hydrogen bonded aggregate, larger than the trimer found with **1b**, appears to be favored with **2b**, where the only difference is the angular displacement of the two complementary groups. This assertion is supported by the ESMS spectrum of **2b** (in methanol; negative ion mode) which showed six major peaks from *m/e* (M−1) to *m/e* (6M−1).

Two possible forms of the larger aggregate with **2b** are shown in Fig. 13. Five molecules linked through 10 hydrogen bonds in a head-to-tail manner can form a cyclic aggregate with a pseudo-planar arrangement of components around a central cavity (Fig. 13a). A similar planarity can be maintained in a linear aggregate (Fig. 13b) resulting in an alternating projection of the alkyl substituents from the central ribbon. The large shifts and sigmoidal shape of the NMR dilution curve for **2b** point to a significant population of the cyclic aggregate that can then undergo a multi-aggregate π-stacking aggregation at higher concentration. In contrast, eliminating the possibility of cyclization (as in **8** and **9**) leads to weaker aggregates and little sigmoidal behavior.

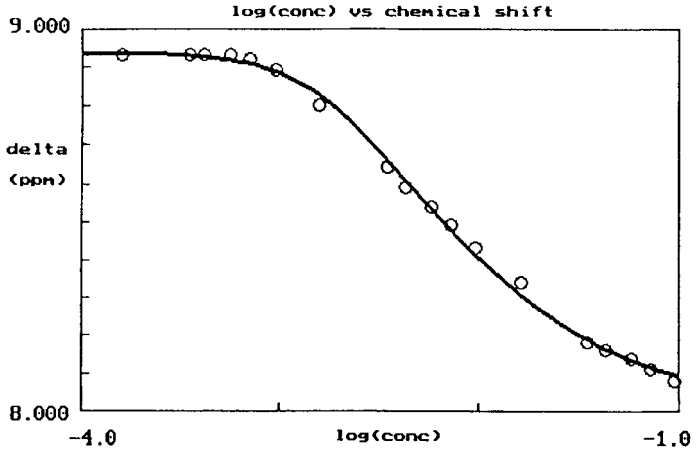

Figure 11. Curve fitting for pyridine-2H in **2b**, with n=3.

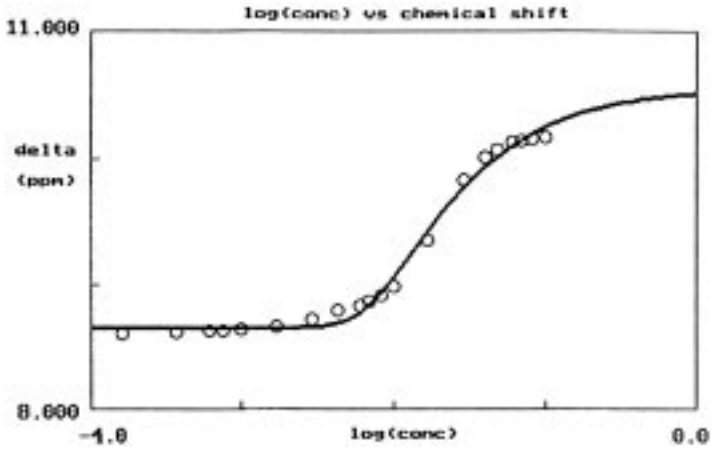

Figure 12. Experimental (○) and calculated (solid line: for n=5) ^{1}H NMR chemical shift of amide-N–H vs log[**2b**] in 2% DMSO-d_6/98% $CDCl_3$ (V/V).

Table 2. The results of curve fitting obtained for the amide N–H at various aggregation numbers (n)

Aggregation number (n)	Aggregation constant (K_n)	Monomer shift δ_m (ppm)	Oligomer shift δ_n (ppm)	$\chi^2\times10^{-3}$
2	13 M^{-1}	8.52	11.89	210.08
3	1376 M^{-2}	8.61	10.88	86.55
4	1.37×10^5 M^{-3}	8.64	10.65	58.96
5	1.40×10^7 M^{-4}	8.65	10.55	55.76
6	1.48×10^9 M^{-5}	8.66	10.49	59.44

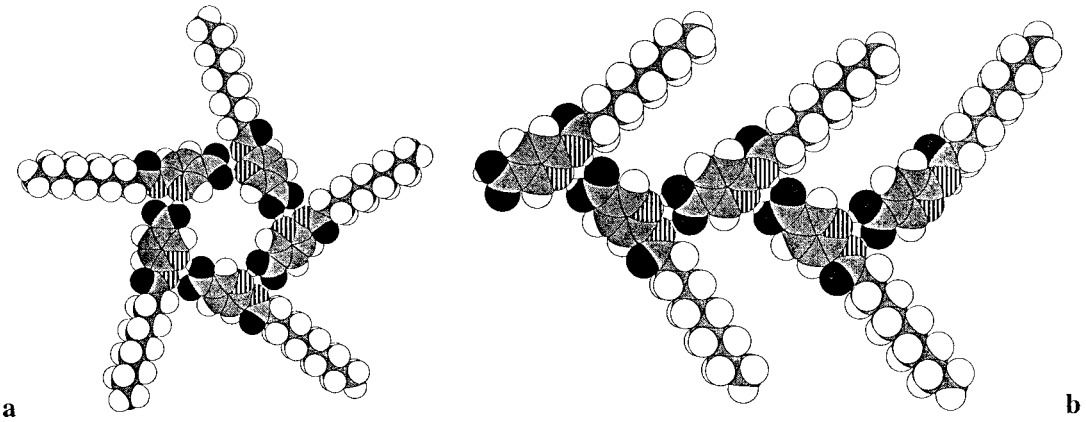

Figure 13. Energy minimized structures of two key aggregation modes in **2b**.[8] (a) Cyclic pentamer. (b) Linear pentamer.

Conclusion

In summary, we have investigated the self-assembling properties of a family of acylaminopyridine–carboxylic acid derivatives. By changing the position of the two hydrogen bonding groups in the molecule we can dramatically change the nature of the aggregate formed in solution. 6-Acylaminopyridine-2-carboxylic acid shows a preference for the formation of trimeric aggregates in solution while 6-acylaminopyridine-3-carboxylic acid forms larger aggregates. ^{1}H NMR and ESMS experiments are used to support the formation of well defined cyclic aggregates in solution.

Experimental

X-ray crystallography was performed on a Siemens R3m/V, Siemens P4 or Rigaku AFC5R spectrometer using Siemens SHELXTL PLUS (PC Version) or Siemens SHELXTL IRIS. The refinement was done by using direct methods on full matrix least-squares fit.

NMR dilution studies were performed in deuterated solvents at room temperature. The dilution data was analyzed by using the Saunders and Hyne model.[13] A computer program was used to determine the best fit for the dilution data at different aggregation numbers. Chi-square values were used as an indicator of the goodness of the fit. The solvents were dried using literature methods. All the chemicals were purchased from Aldrich except 6-aminonicotinic acid which was purchased from Lancaster Chemicals. Proton and ^{13}C NMR spectra were recorded on a Bruker AM-300 (300 MHz) instrument. NMR chemical shifts are reported in ppm downfield from tetramethylsilane (TMS). EI and FAB

mass spectra (MS) were obtained using a Varian MAT CH-5 or VG 7070 mass spectrometer under the direction of Dr Kasi V. Somayajula in the Department of Chemistry at the University of Pittsburgh. Melting points were determined using an Electrothermal capillary melting point apparatus. Elemental analysis was carried out by Atlantic Microlab, Inc. Norcross, GA.

2-Acetylamino-6-methylpyridine (5). To a solution of 2-amino-6-picoline (5.0 g, 46.23 mmol) in dichloromethane (100 mL) at 0°C was added acetic anhydride (4.9 mL, 50.86 mmol). The solution was stirred for 12 h at room temperature and then the solvent was evaporated under reduced pressure. The resulting light yellow solid was dried under vacuum for 18 h. The dry product was dissolved in potassium hydroxide solution (3.2 g, 57.03 mmol). The solution was extracted with dichloromethane (2×40 mL) and the combined organic extract was dried over anhydrous magnesium sulfate. The solvent was evaporated under reduced pressure and the residue was dried under vacuum to obtain a light yellow crystalline solid as the desired product (6.3 g, 90.7%): mp 86–88°C; ^{1}H NMR (300 MHz, $CDCl_3$) δ 8.25 (1H, br s, amide N–H), 7.97 (1H, d, J=8.1 Hz, Pyr. C–H at C-3), 7.57 (1H, t, J= 7.8 Hz, Pyr. C–H at C-4), 6.87 (1H, d, 7.5 Hz, Pyr. C–H at C-5), 2.42 (3H, s, Pyr–CH_3), 2.15 (3H, s, acetyl CH_3); ^{13}C NMR (75 MHz, $CDCl_3$) δ 169.5, 156.3, 150.8, 138.4, 118.9, 111.0, 24.2, 23.7; HRMS *m/e* calcd for $C_8H_{10}N_2O$: 150.0793, found 150.0789.

6-Acetylaminopyridine-2-carboxylic acid (1a). 2-Acetylamino-6-picoline (2.86 g, 19 mmol) was dissolved in water (50 ml) and the solution was heated to 70°C. Potassium permanganate (6.32 g, 39 mmol) was added in small increments over a period of 30 min. The solution was refluxed for 5 min and filtered. The residue was washed several times with boiling water. The washings and the filtrate were combined and the volume was decreased to 50 ml on the rotary evaporator. The solution was acidified to pH ~1.5 by using concentrated hydrochloric acid and then the pH was adjusted to ~4.5 by adding saturated sodium bicarbonate solution. After 2 h of refrigeration the precipitate was filtered, washed with water and air dried to obtain a light yellow powder as the desired product (0.88 g, 26%): mp 215–217°C; ^{1}H NMR (300 MHz, DMSO-d_6) δ 11.80 (1H, br, acid OH), 10.79 (1H, s, amide N–H), 8.26 (1H, d, J=8.4 Hz, Pyr. C–H at C-3), 7.92 (1H, t, J=8.1 Hz, Pyr. C–H at C-4), 7.71 (1H, d, J=7.5 Hz, Pyr. C–H at C-5), 2.09 (3H, s, acetyl CH_3); ^{13}C NMR (75 MHz, DMSO-d_6) δ 169.8, 165.9, 152.0, 146.9, 139.3, 120.1, 116.8, 23.9; HRMS *m/e* calcd for $C_8H_8N_2O_3$: 180.0534, found 180.0524.

6-Aminopyridine-2-carboxylic acid ethyl ester (6). A 100 mL round bottom flask, fitted with a reflux condenser and a drying tube (drierite), was charged with 6-aminopyridine-2-carboxylic acid (0.50 g, 3.61 mmol) and an excess of oxalyl chloride (10 mL). The reaction mixture was stirred at room temperature for 12 h and then at 45°C for 1 h. The solvent was evaporated on a rotary evaporator. The residue was dried under vacuum for about 1/2 h. Absolute ethanol (70 mL) was then added slowly (caution). The resulting suspension was refluxed for 1 h. The solvent was removed on a rotary evaporator and the residue was suspended in a mixture of water (25 mL) and saturated sodium bicarbonate (20 mL). The aqueous suspension was then extracted with diethyl ether (6×15 mL). The combined ether extract was dried over anhydrous magnesium sulfate. The solution was concentrated by rotary evaporation and after 12 h, the crystalline product was filtered and washed with a minimum amount of cold (−20°C) diethyl ether (0.50 g, 84%): mp 70–71°C; ^{1}H NMR (300 MHz, $CDCl_3$) δ 7.43 (1H, t, J=7.6 Hz, Pyr. C–H at C-4), 7.36 (1H, d, J=6.8 Hz, Pyr. C–H at C-3), 6.59 (1H, d, J=7.9 Hz, Pyr. C–H at C-5), 5.20 (2H, s, NH_2), 4.33 (2H, q, J=7.1 Hz, OCH_2), 1.32 (3H, t, J=7.1 Hz, ester CH_3); ^{13}C NMR (75 MHz, $CDCl_3$) δ 166.3, 159.6, 147.1, 138.9, 116.0, 113.5, 62.3, 15.1; MS *m/e* calcd for $C_8H_{10}N_2O_2$: 166.0742, found 166.0744.

6-Decanoylaminopyridine-2-carboxylic acid ethyl ester (7). To a solution of **6** (0.76 g, 4.58 mmol) in dichloromethane (50 mL) was added decanoyl chloride (0.95 mL, 4.58 mmol). The reaction mixture was stirred at room temperature for 18 h and then water (15 mL) and saturated sodium bicarbonate were added (2 mL). The organic layer was separated and the aqueous layer was extracted again with dichloromethane (25 mL). The combined organic extract was dried over anhydrous magnesium sulfate. The solvent was then removed on a rotary evaporator and the residue was dried under vacuum to give the crude product. The crude material was purified by silica gel chromatography using a mixture of ethyl acetate and hexane (1:1) to afford the desired product (1.15 g, 78%): mp 42–44°C; ^{1}H NMR (300 MHz, $CDCl_3$) δ 8.47–8.41 (1H, m, Pyr. C–H at C-3), 8.28 (1H, s, amide N–H), 7.85–7.80 (2H, m, Pyr. C–H at C-4 and C-5), 4.46 (2H, q, J=7.1 Hz, ester CH_2), 2.38 (2H, t, J=7.4 Hz, N–$COCH_2$), 1.77–1.61 (2H, m, N–$COCH_2$–CH_2), 1.42 (3H, t, J=7.1 Hz, ester CH_3), 1.31–1.26 (12H, br m, alkyl chain), 0.86 (3H, t, J= 6.2 Hz, alkyl chain CH_3); ^{13}C NMR (75 MHz, $CDCl_3$) δ 172.4, 164.8, 151.7, 146.2, 139.5, 121.0, 117.8, 62.2, 37.9, 32.0, 29.4, 25.5, 22.8, 14.4, 14.3; MS *m/e* calcd for $C_{18}H_{28}N_2O_3$: 320.2099, found 320.2100.

6-Decanoylaminopyridine-2-carboxylic acid (1b). To a suspension of **7** (0.79 g, 2.48 mmol) in a mixture of water and ethanol (31 mL, 1:4) was added lithium hydroxide monohydrate (0.10 g, 2.48 mmol). The reaction mixture was stirred at room temperature for 30 h. In order to complete the reaction another portion of lithium hydroxide monohydrate (0.04 g, 0.95 mmol) was added. The reaction mixture was then refluxed for 1 h and then the solvent was removed on a rotary evaporator. The residue was then dissolved in water (20 mL) and filtered. The pH of aqueous solution was then adjusted to 4.9 and the white precipitate were filtered, washed thoroughly with water and air dried to isolate the crude product. The crude material was purified by silica gel chromatography using 10% methanol in dichloromethane as the eluant to afford shiny thin needles as the product (0.25 g, 35%): mp 102–103°C; ^{1}H NMR (300 MHz, THF-d_8) δ 10.90 (1H, s, acid OH), 9.94 (1H, s, amide N–H), 8.44 (1H, d, J=7.8 Hz, Pyr. C–H at C-3), 7.81 (1H, t, J=7.5 Hz, Pyr. C–H at C-4), 7.73 (1H, d, J=7.5 Hz, Pyr. C–H at C-5), 2.40 (2H, t, J=6.9 Hz, N–$COCH_2$), 1.72 (embedded under the solvent peak), N–CH_2CH_2), 1.34–1.28 (br m, 14H, alkyl chain), 0.88 (3H, t, J=6.9 Hz, alkyl

CH_3); ^{13}C NMR (75 MHz, DMSO-d_6) δ 172.7, 166.1, 151.8, 139.2, 119.8, 116.4, 36.0, 31.3, 28.7, 24.9, 22.1, 13.8; MS *m/e* calcd for $C_{16}H_{24}N_2O_3$: 292.1786, found 292.1776.

6-Acetylaminopyridine-3-carboxylic acid (2a). To a solution of 6-aminonicotinic acid (1.0 g, 7.24 mmol) in pyridine (30 mL) was added acetic anhydride (0.81 mL, 7.96 mmol) and the reaction mixture was heated at 130°C for 24 h. The reaction mixture was then cooled to room temperature and the white precipitate was filtered and washed with pyridine and excess water. The white solid was dried under vacuum to afford the desired product (1.2 g, 92%): mp 281° (decomp.); ^1H NMR (300 MHz, DMSO-d_6) δ 10.85 (1H, s, amide N–H), 8.79 (1H, d, J=2.1 Hz, Pyr. C–H at C-2), 8.21–8.14 (2H, m, Pyr. C–H at C-4 and C-5), 2.11 (3H, s, acetyl CH_3); ^{13}C NMR (75 MHz, DMSO-d_6) δ 169.8, 166.0, 155.0, 149.7, 139.4, 121.9, 112.3, 24.0; MS *m/e* calcd for $C_8H_8N_2O_3$: 180.0534, found 180.0540.

6-Decanoylaminopyridine-3-carboxylic acid (2b). 6-Aminonicotinic acid (0.50 g, 3.61 mmol) was dissolved in pyridine at 70°C under nitrogen. Decanoyl chloride (1.6 mL, 7.2 mmol) was added over a period of 45 min. The solution was heated to 110°C for 6 h. Water (50 mL) was added to the solution and it was acidified to pH ~4 by using hydrochloric acid (6 M). The precipitate was filtered and washed thoroughly with water and air dried. The solid was washed with hexane and dichloromethane and dried under vacuum to obtain a white powder as the desired product (0.59 g, 57%): mp 205°C (Decomp.); ^1H NMR (300 MHz, DMSO-d_6) δ 12.00 (1H, br, acid OH), 10.79 (1H, s, amide N–H), 8.79 (1H, s, Pyr. C–H at C-2), 8.21 (2H, m, Pyr. C–H at C-4 and C-5), 2.39 (2H, t, J=7.2 Hz, $NCOCH_2$), 1.56 (2H, m, $NCOCH_2$–CH_2), 1.22 (12H, br, alkyl chain CH_2), 0.83 (3H, t, J=6.9 Hz, alkyl chain CH_3); ^{13}C NMR (75 MHz, DMSO-d_6) δ 172.8, 165.9, 155.1, 149.6, 142.9, 139.3, 121.6, 112.3, 36.1, 31.3, 28.7, 28.6, 24.8, 22.1, 13.9; MS *m/e* calcd for $C_{16}H_{24}N_2O_3$: 292, found 292.

Acknowledgements

This work was supported by a grant from the National Science Foundation.

References

1. (a) Klok, H.-A.; Jolloffe, K. A.; Schauer, C. L.; Prins, L. J.; Spatz, J. P.; Möller, M.; Timmerman, P.; Reinhoudt, D. N. *J. Am. Chem. Soc.* **1999**, *121*, 7154–7155. (b) Kolotuchin, S. V.; Zimmerman, S. C. *J. Am. Chem. Soc.* **1998**, *120*, 9092–9093. (c) Conn, M. M.; Rebek, Jr., J. *Chem. Rev.* **1997**, *97*, 1647–1668. (d) Marsh, A.; Silvestri, M.; Lehn, J. M. *Chem. Commun.* **1996**, 1527–1528. (e) Fredericks, J. R.; Hamilton, A. D. In *Comprehensive Supramolecular Chemistry*, 1st ed.; Atwood, J. L., Davies, J. E. D., MacNicol, D. D., Vogtle, F., Eds.; Elsevier Science: New York, 1996; Vol. 9, pp 565–593. (f) Lawrence, D. S.; Jiang, T.; Levett, M. *Chem. Rev.* **1995**, *95*, 2229–2260, (g) Whitesides, G. M.; Simanek, E. E.; Mathias, J. P.; Seto, C. T.; Chin, D. N.; Mammen, M.; Gordon, D. M. *Acc. Chem. Res.* **1995**, *28*, 37–54.

2. Rebek Jr., J. *Chem. Soc. Rev.* **1996**, 225–264.

3. Cram, D. J. *Angew. Chem. Int. Ed. Engl.* **1988**, *27*, 1009–1112.

4. Garcia-Tellado, F.; Geib, S. J.; Goswami, S.; Hamilton, A. D. *J. Am. Chem. Soc.* **1991**, *113*, 9265–9269.

5. Yang, J.; Fan, E.; Geib, S. J.; Hamilton, A. D. *J. Am. Chem. Soc.* **1993**, *115*, 5314–5315.

6. Jones, R. E.; Templeton, D. H. *Acta Crystallogr.* **1958**, *11*, 484.

7. Clark, T. D.; Buriak, J. M.; Kobayashi, K.; Isler, M. P.; McRee, D. E.; Ghadiri, M. R. *J. Am. Chem. Soc.* **1998**, *120*, 8949–8962.

8. Zimmerman, S. C.; Duerr, B. F. *J. Org. Chem.* **1992**, *57*, 2215–2217.

9. Molecular modeling was done using the Amber forcefield and a continuum dielectric for chloroform within the MacroModel program. Still, W.C., Columbia University.

10. We were unable to detect the amide N–H below 1 mM due to broadening.

11. Zhang, J.; Moore, J. S. *J. Am. Chem. Soc.* **1992**, *114*, 9701–9702.

12. Yang, J.; Marendez, J. L.; Geib, S. J.; Hamilton, A. D. *Tetrahedron Lett.* **1994**, 3665–3668.

13. Saunders, M.; Hyne, J. B. *J. Chem. Phys.* **1958**, *20*, 1319–1323.